

Large perpendicular magnetic anisotropy in magnetostrictive $\text{Fe}_{1-x}\text{Ga}_x$ thin films

M. Barturen,^{1,2,3,4,5} J. Milano,^{1,2,5} M. Vázquez-Mansilla,¹ C. Helman,^{5,6}

M. A. Barral,^{5,6} A. M. Llois,^{5,6} M. Eddrief,^{3,4,5} and M. Marangolo^{3,4,5}

¹CNEA-CONICET, Centro Atómico Bariloche, (R8402AGP) San Carlos de Bariloche, Argentina

²Instituto Balseiro, Universidad Nacional de Cuyo,

Centro Atómico Bariloche, (R8402AGP) San Carlos de Bariloche, Argentina

³Sorbonne Universités, UPMC Univ Paris 06, UMR 7588, INSP, 4 place Jussieu, F-75005, Paris, France

⁴CNRS, UMR 7588, Institut des Nanosciences de Paris, 4 place Jussieu, F-75005, Paris, France

⁵LIFAN, Laboratorio Internacional Franco-Argentino en Nanociencias

⁶CNEA, Centro Atómico Constituyentes, Avenida General Paz 1499, San Martín, Argentina

(Dated: March 7, 2018)

In this work we report the appearance of a large perpendicular magnetic anisotropy (PMA) in $\text{Fe}_{1-x}\text{Ga}_x$ thin films grown onto $\text{ZnSe}/\text{GaAs}(001)$. This arising anisotropy is related to the tetragonal metastable phase in as-grown samples recently reported [M. Eddrief *et al.*, Phys. Rev. B **84**, 161410 (2011)]. By means of ferromagnetic resonance studies we measured PMA values up to $\sim 5 \times 10^5$ J/m³. PMA vanishes when the cubic structure is recovered upon annealing at 300°C. Despite the important values of the magnetoelastic constants measured via the cantilever method, the consequent magnetoelastic contribution to PMA is not enough to explain the observed anisotropy values in the distorted state. *Ab initio* calculations show that the chemical ordering plays a crucial role in the appearance of PMA. Through a phenomenological model we propose that an excess of next nearest neighbour Ga pairs (B₂-like ordering) along the perpendicular direction arises as a possible source of PMA in $\text{Fe}_{1-x}\text{Ga}_x$ thin films.

I. INTRODUCTION

Nowadays, active research efforts are being carried out to stabilize perpendicular magnetic anisotropy (PMA) in thin films and nanostructures because it is at the intersection of different research streams of modern magnetism and spintronics. An example is the spin transfer torque - magnetic random access memory (STT-MRAM) where magnetized units are more easily switched by a lower electrical current when the electrodes present PMA.^{1,2} The PMA tends to align the magnetic moments within the film perpendicular to the film surface. To achieve this goal, different approaches have been adopted based on very different physical phenomena. PMA can be obtained by magnetocrystalline anisotropy (MCA) (such as in Co),³ interface effects,⁴ stress^{5,6} and shape of the magnetic entities.⁷ In particular, magnetocrystalline effects can be used for obtaining PMA in materials with a preferential crystalline axis. This is the case of Co when its easy axis is along the film growth direction (perpendicular to the film surface).⁸ Furthermore, it is possible to manipulate the crystallographic structure and to induce an easy axis of the magnetization by adjusting the growing conditions or postdeposition treatments. This is the case of the L1₀-ordered alloys, whose particular chemical ordering is reached by thermal annealing or by high temperature thin film growth.⁹ The tetragonal distortion induced by the atomic arrangement is responsible for the appearance of the PMA.¹⁰ An example of these alloys is FePt which presents a very high PMA, i.e. $\sim 3\text{--}7 \times 10^6$ J/m³.^{11,12} However, it is worthwhile to report that more "moderate" PMA values are needed to obtain lower switching fields in recording applications. This motivates the study of the L1₀-ordered FePd alloys where PMA is

$\sim 1 \times 10^6$ J/m³.¹³

In this work, we report the presence of PMA in $\text{Fe}_{1-x}\text{Ga}_x/\text{ZnSe}/\text{GaAs}(001)$ thin films. A combined experimental and theoretical study of such films as a function of the Ga content and the atomic ordering was performed. The PMA was deduced from ferromagnetic resonance (FMR) experiments and large values up to $\sim 5 \times 10^5$ J/m³ are found. Due to demagnetization fields, the magnetization lies in the film plane of our samples; however the measured PMA values assure that the magnetization is perpendicular to the film plane when the lateral size is smaller than ~ 130 nm.¹⁴ By taking inspiration from a phenomenological model proposed for bulk $\text{Fe}_{1-x}\text{Ga}_x$,¹⁵ we estimate the contribution of Ga ordering to magnetic anisotropy energy (MAE) due to PMA. This permits us to suggest that the strong PMA is due to a preferential Ga ordering along the growth direction. Our first-principles calculations in the framework of density functional theory account for the role played by Ga ordering. The experimental observation of "moderate" PMA is of considerable interest for the following reasons: (i) $\text{Fe}_{1-x}\text{Ga}_x$ (Galfenol) is a material well known for its very high magnetostrictive coefficient and its growth is well mastered by today's industry; (ii) Epitaxial films of $\text{Fe}_{1-x}\text{Ga}_x$ on GaAs present spintronic properties like spin injection into a semiconductor,¹⁶ strain-tuned magnetic anisotropy and high frequency properties in the microwave region;¹⁷ (iii) PMA is obtained without any annealing procedure and at moderate growth temperature compatible with ferromagnetic/semiconductor heterostructures engineering. In addition to all of these advantages, at present, Ga has a lower cost than Pt or Pd due to its crustal abundance.¹⁸

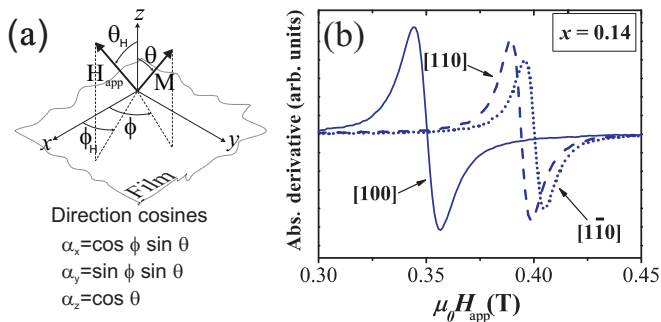


FIG. 1. (Color online) (a) Coordinate system used in Eqs. (1) and (2). (b) FMR spectra for different directions of H_{app} for the $\text{Fe}_{0.86}\text{Ga}_{0.14}$ sample.

II. EXPERIMENTAL

Epitaxial $\text{Fe}_{1-x}\text{Ga}_x$ samples were grown by Molecular Beam Epitaxy on $c(2\times 2)$ Zn-terminated ZnSe epilayers onto GaAs(001) substrates.^{19,20} At the end, the films were covered by a protective 3-nm gold capping layer. Details of the growth are given in Ref. 21. We fabricated 72-nm nominal thick samples at several Ga concentrations, $x = 0.14, 0.18, 0.20$. Such concentrations were determined by means of x-ray photoelectron spectroscopy (XPS) and confirmed by Rutherford backscattering (RBS) and energy dispersive x-ray spectrometry (EDX). With the aim to study the response to thermal treatment, a selection of samples of varying Ga concentration (for $x = 0.14$ and 0.20) were annealed at 300°C in ultra high vacuum²¹ as well. This annealing temperature is sufficient to cause Ga mobility in the Fe matrix, as attested in Ref. 22 and, at the same time, it preserves the sharp FM/SC interface.¹⁹ By X-ray diffraction (XRD), we determine the lattice parameters and we observe a Ga dependent tetragonal deformation. Ref. 21 suggests that this deformation is due to Ga pairing along $[001]$ direction leading to a local B_2 -like structure as foreseen by previous *ab initio* studies^{23,24} and experimentally observed by differential x-ray absorption spectroscopy (DiffXAS).²⁵ Such a B_2 -like phase occurs when Ga pairs are formed at next nearest neighbours along the $\langle 100 \rangle$ family direction. The first magnetic characterizations put in evidence clearly the presence of PMA where the formation of stripe-like domains is reported.^{26,27} We performed FMR experiments in a Bruker ESP-300 spectrometer at $\nu \sim 24$ GHz (K-band). The angular dependence of the resonance spectra has been studied in the in-plane geometry by fixing the polar angle at $\theta_H = 90^\circ$ while varying ϕ_H from 0° to 360° [see Fig. 1(a)]. We also measured the magnetoelastic coupling by performing cantilever deflection experiments. The magnetic field was applied along the $[100]$ direction in order to obtain the magnetoelastic coupling along such direction. Additional magnetization measurements have been performed in a superconducting quantum interference device (SQUID) and a vibrating

sample magnetometer (VSM).

III. RESULTS AND DISCUSSION

In order to study quantitatively the magnetic anisotropies in our samples through FMR, we evaluate how these anisotropies contribute to the resonance field, H_r . To do this, we propose a self-consistent scheme that solves the equilibrium position of \mathbf{M} via the magnetic free energy U and a linearized version of the Landau-Ginzburg equation of motion for the magnetization,²⁸ when the sample is magnetically saturated. It is important to notice that the onset of a tetragonal distortion along z -axis modifies the well-known cubic anisotropy energy term of pure Fe thin films, i.e. the cubic term $[K_4^{\text{Fe}}(\alpha_x^2\alpha_y^2 + \alpha_y^2\alpha_z^2 + \alpha_z^2\alpha_x^2)]$ is modified as $K_4^{\text{IP}}\alpha_x^2\alpha_y^2 + K^{\text{OP}}\alpha_z^2$, where the out-of-plane α_z^4 -term was neglected. α_i denotes the direction cosines of the magnetization [Fig. 1(a)] and IP (OP) is the in-plane (out-of-plane) direction. Hence, the proposed expression for U in our coordinate system [Fig. 1(a)] is the following:

$$U(\theta, \phi) = -\mu_0 \mathbf{H}_{\text{app}} \cdot \mathbf{M} + \frac{\mu_0}{2} M^2 \cos^2 \theta \quad (1) \\ + \frac{1}{4} K_4^{\text{IP}} \sin^4 \theta \sin^2 2\phi - K_{\text{PMA}} \cos^2 \theta \\ + K_u \sin^2 \theta \cos^2 \left(\phi - \frac{\pi}{4} \right)$$

where \mathbf{H}_{app} is the applied magnetic field, \mathbf{M} is the magnetization vector, μ_0 is the vacuum permeability ($\mu_0 = 4\pi \times 10^{-7}$ T m/A). The first term on the right-hand side is the classical Zeeman energy. The second one is the energy related to the demagnetizing dipolar field. The third term is the first order in-plane contribution to the magnetocrystalline energy for a tetragonal lattice. The fourth one is the energy related to the PMA, including K^{OP} and other contributions that will be discussed below. Finally, the fifth term stands for an uniaxial in-plane anisotropy arising from the $\text{Fe}_{1-x}\text{Ga}_x/\text{ZnSe}$ interface. On the other hand, the equation that accounts for the magnetization dynamics in the small oscillation approximation was given by Smit and Beljers²⁸ and it writes:

$$\omega^2 = \frac{\gamma^2}{M^2 \sin^2 \theta} \left[\frac{\partial^2 U}{\partial^2 \theta} \frac{\partial^2 U}{\partial^2 \phi} - \left(\frac{\partial^2 U}{\partial \theta \partial \phi} \right)^2 \right] \Bigg|_{\theta_{eq}, \phi_{eq}}, \quad (2)$$

evaluated at the equilibrium angles, θ_{eq} and ϕ_{eq} obtained from Eq. (1), where $\gamma = g\mu_B/\hbar$ is the gyromagnetic ratio and μ_B is the Bohr magneton. The g value was set to 2.1, as for Fe.

In Fig. 1(b), we show an example of spectra taken at different H_{app} in-plane directions. The shift of the resonance mode is due to the magnetic anisotropies present in the samples. It is worth to note that even though H_{app} is applied only in the film plane, it is possible to extract

information of the perpendicular anisotropy.²⁹ The magnetic parameters, i.e. K_{PMA} , K_4^{IP} and K_u , are determined by solving self-consistently the Eqs. (1) and (2) as mentioned above. In Fig. 2(a), we show K_4^{IP} as a function of Ga concentration. The K_4^{IP} behavior is similar to the one observed in $\text{Fe}_{1-x}\text{Ga}_x$ bulk:¹⁵ (i) It decreases for increasing Ga concentrations and (ii) it changes its signs. In Fig. 2(b), K_u vs. x is shown. This contribution arises from the dangling bonds at the $\text{Fe}_{1-x}\text{Ga}_x/\text{ZnSe}$ interface as already seen in Fe/ZnSe interfaces.^{30,31} K_u diminishes for increasing x . This behavior is probably due to the fact that amount of Fe atoms at the interface decreases for higher Ga concentrations.

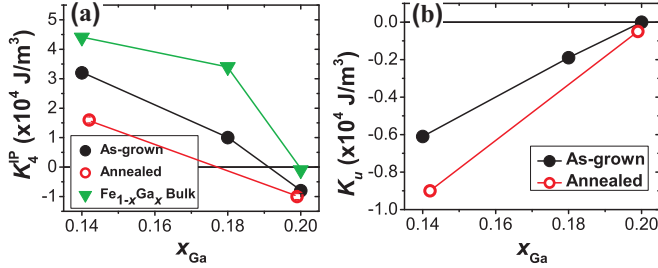


FIG. 2. (Color online) (a) K_4^{IP} and (b) K_u as a function of x .

In the following, we focus our analysis on K_{PMA} and Fig. 3(a) displays the best fitted values for it. It is important to note the difference between the results obtained for the as-grown and the annealed samples. On one hand, the as-grown samples show very high values of K_{PMA} being the highest value $\sim 5 \times 10^5 \text{ J/m}^3$ at $x = 0.20$, i.e. 10 times larger than pristine Fe thin films. On the other hand, for the annealed samples, K_{PMA} shows values close to zero. This indicates that the appearance of K_{PMA} is related to the tetragonal deformation. Fig. 3(b) displays K_{PMA} as a function of the c/a ratio (which measures the tetragonal deformation), where the correlation between them is explicitly shown.

In what follows, we discuss possible sources of PMA for our systems. In distorted ferromagnetic systems, a contribution that cannot be discarded is the one arising from magnetoelasticity, specially if the studied system is highly magnetostrictive as in the case of $\text{Fe}_{1-x}\text{Ga}_x$. Hence, the magnetoelastic contribution to K_{PMA} of an out-of-plane tetragonally distorted ($\epsilon_{yy}=\epsilon_{xx}$) film writes:³²

$$K_{\text{PMA}}^{\text{ME}} = B_1(\epsilon_{zz} - \epsilon_{xx}), \quad (3)$$

where B_1 is the magnetoelastic constant related to tetragonal strains. ϵ_{zz} (ϵ_{xx}) is the strain along the z (x) direction. In order to determine if K_{PMA} in our distorted systems comes from the magnetoelastic coupling, we evaluate Eq. (3) for a given concentration. We consider ϵ_{zz} (ϵ_{xx}) being equal to $\frac{c-a_{\text{cub}}}{a_{\text{cub}}}$ ($\frac{a-a_{\text{cub}}}{a_{\text{cub}}}$), where a_{cub} is the cubic lattice parameter extracted from the stabilized cubic phase (annealed samples).³³ B_1 was measured

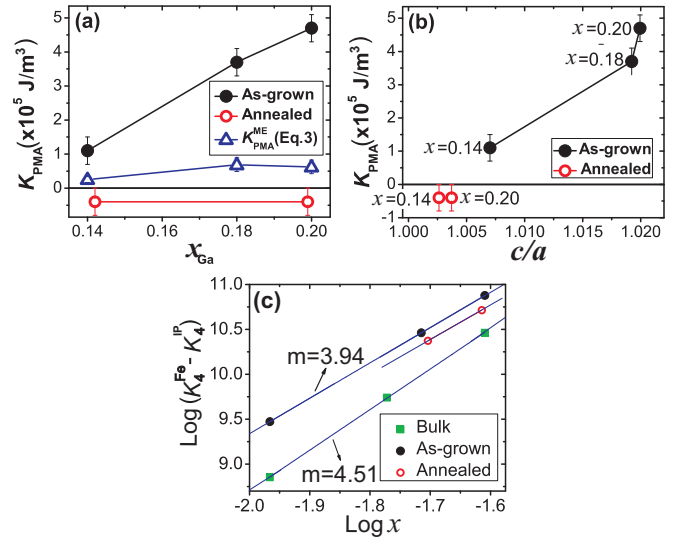


FIG. 3. (Color online) (a) K_{PMA} as a function of x . (b) K_{PMA} as a function of c/a . (c) Log-Log plot of $(K_4^{\text{Fe}} - K_4^{\text{IP}})$ vs. x , where the slopes show explicitly the x^4 dependence. The K_4^{IP} for the cubic symmetry dependence of bulk $\text{Fe}_{1-x}\text{Ga}_x$ taken from Ref. 15 is shown as well.

at MPI (Halle, Germany) for the cubic samples by performing cantilever deflection experiments,^{34,35} which provide a direct measurement of the magnetoelastic coupling coefficients in our films. The maximum value reported by us is $B_1 = (5 \pm 1) \times 10^6 \text{ J/m}^3$ for $x = 0.14$. In Fig. 3(a), we show the calculated $K_{\text{PMA}}^{\text{ME}}$ via Eq. (3). We observe that $K_{\text{PMA}}^{\text{ME}}$ is only a small fraction of K_{PMA} and, therefore, the PMA anisotropy observed by FMR does not arise from a simple structural deformation. Consequently, we conclude that another source of PMA dominates in our system. In that sense, we propose that the observed PMA has a magnetocrystalline origin linked to the preferential Ga ordering along the $[001]$ direction. Indeed, it is well known that Ga-ordering strongly affects MCA in bulk $\text{Fe}_{1-x}\text{Ga}_x$. Cullen *et al.* have shown the Ga-pairing along $\langle 100 \rangle$ directions (second nearest neighbors) lowers the magnetocrystalline anisotropy of pristine bulk iron (K_4^{Fe}) in the following way:

$$K_4^{\text{IP}} = K_4^{\text{Fe}} - AK^2x^4, \quad \text{with } A = 4a^2/\pi A_0. \quad (4)$$

Where K_4 is the magnetocrystalline anisotropy observed in $\text{Fe}_{1-x}\text{Ga}_x$, A_0 is the exchange stiffness constant and a is related to the size of the Ga arrangement, in our case equals one lattice parameter. Such a parameter “measures” how the Ga atoms affect the magnetic properties of the surrounding Fe atoms. K gives account for a local uniaxial anisotropy due to the presence of the Ga pairs. Here, we take $A_0 = 1.6 \times 10^{-11} \text{ J/m}^3$ consistently with reported values for similar films.³⁶ The core of this phenomenological model is that such Ga pairs aligned along the $\langle 100 \rangle$ axes lead to an extra contribution to the free energy that takes into account the tendency for the spin

of the neighboring Fe atoms to align, in principle, parallel or perpendicular to the Ga-Ga pair axes. This energy term reads as follows:

$$U_{\text{pair}}^0 = \frac{K}{N} \sum_l \sum_i \alpha_i^2(R_l) P_{0,i}(R_l). \quad (5)$$

Where N is the number of sites, $\alpha_i(R_l)$ indicates the local R_l -site magnetization directions with respect to the i^{th} ($i = x, y, z$) axis and $P_{0,i}(R_l)$ is the probability (0 or 1) that the Ga pairs in the R_l site are aligned along the i^{th} axis. Eq. (4) can be also recovered from Eq. (5) in a mean-field approach^{15,37}. Results obtained in Ref. 15 for bulk $\text{Fe}_{1-x}\text{Ga}_x$ (which will be useful to compare to our results) are shown in Fig. 3(c) where a $\sim x^4$ dependence is observed. A fitting procedure gives $K \sim 2.9 \times 10^7 \text{ J/m}^3$.

In the following we will show how, given an anisotropic distribution of Ga pairs along the three $\langle 100 \rangle$ direction, the previously reported K values can lead to the observed PMA. As a starting point we propose that the Ga pairs are preferentially aligned along the [001] out of plane direction rather than in plane. This hypothesis is supported by the experimentally observed tetragonal distortion leading to the B_2 -like structure mentioned before, coherently with *ab initio* calculations.^{23,24} Consequently, we propose that the total probability of finding a Ga pair at the R_l -site can be expressed as

$$P_i(R_l) = P_{0,i}(R_l) + P_z(R_l) \delta_{iz}, \quad (6)$$

where P_z accounts for the additional probability of finding Ga pairs along the z axis, which is expressed through δ_{iz} . We notice that for cubic $\text{Fe}_{1-x}\text{Ga}_x$ (bulk or annealed samples), $P_z = 0$. On the other hand, for a tetragonal distorted crystal Eq. (5) becomes:

$$U_{\text{pair}}^z = U_{\text{pair}}^0 + \frac{K}{N} \sum_l \alpha_z^2(R_l) P_z(R_l). \quad (7)$$

Under this scheme the PMA anisotropy is obtained as

$$K_{\text{PMA}} = U_{\text{pair}}(\alpha_z = 1, P_{0,i}, P_z) - U_{\text{pair}}(\alpha_z = 0, P_{0,i}, P_z) \\ = K P_z, \quad \text{where } P_z = \frac{\sum_l P_z(R_l)}{N}. \quad (8)$$

In Fig. 3(c), we display $\log(K_4^{\text{Fe}} - K_4^{\text{IP}})$ vs. $\log x$ where the dependency on the fourth power of the Ga concentration corroborates the extension of the Cullen's model to the tetragonally distorted thin films. A similar behavior is recovered for the two annealed samples, as well. The important point is that the in-plane measurements permit us to estimate $K \sim 3.6 \times 10^7 \text{ J/m}^3$, slightly higher than in bulk, adopting the same A value.

For $x = 0.20$, a lower limit for $\langle P_{0,i} \rangle$ can be calculated using the results of the *ab initio* molecular dynamics simulations performed in Ref. 38, from which it is possible to determine the amount of B_2 -like pairs for a given concentration. Those calculations foresee that the number of B_2 -pairs is very small, i.e. only 1% of

the D0_3 (the majority phase existing in $\text{Fe}_{1-x}\text{Ga}_x$ alloys) pairs. An upper limit is obtained by considering a fully random distribution of the Ga atoms into the bcc Fe matrix (x^2), i.e. $\langle P_{0,i} \rangle \sim x^2 \sim 0.04$.³⁷ It is important to notice that X-ray diffraction experiments²¹ attest the presence of superlattice reflections (B_2 or D0_3) but the absence of the D0_3 -characteristic [113] reflections. Consequently we estimate that the aforementioned lower limit is not encountered in our metastable thin films and that $P_{0,x} + P_{0,y} + P_{0,z}$ is close to the upper limit, i.e. $\sim 10\%$. Moreover, the observed tetragonal distortion suggests an anisotropic distribution of Ga atoms, with a preferential axis along [001]. Even if we are not able to measure the exact Ga-Ga pairs distribution in our films, we notice that the K value estimated above is so huge that a small P_z unbalance of few 10^{-2} can lead to a K_{PMA} close to the observed experimental values of $5 \times 10^5 \text{ J/m}^3$, for $x = 0.20$. This phenomenological approach allows us to conclude that K_{PMA} can be favored if there is an anisotropic distribution of Ga pairs between in-plane and out-of-plane directions. However, from this approximation it is not possible to determine which is the preferential orientation of the pairs that gives rise to the PMA.

In this context, from a more microscopical point of view, *ab initio* calculations within the framework of density functional theory (DFT) can provide an insight into the Ga pairing effect on PMA in order to: (i) predict the direction of the local easy axis with respect to the Ga pairs direction; (ii) estimate the intensity of MAE induced by Ga atoms alignment. The MAE is calculated, using a second variational approach as implemented in the Wien2k package.^{39,40} The pairs are built by Ga atoms located at next nearest neighbour positions in the bcc lattice of Fe and directed along [001] direction. The in-plane lattice constant, perpendicular to the Ga pairs, is set equal to the Fe lattice one, as experimentally observed in our samples (see Ref. 21). The system is allowed to relax in the out-of-plane direction. As we stated above the dependence of K with the arrangement of Ga pairs (a in Eq. 4) has to be considered. In order to take that into account in the calculations, we proposed two situations where the Ga pairs are along [001] but are placed in different manners as it is shown in the insets of Fig. 4. In one case single pairs arrangement is assumed (right inset); in the second case, the Ga pairs build chains (left inset). The Ga concentrations of both structure are similar to the ones measured in the studied samples, i.e. $x \sim 0.16$ and $x \sim 0.12$ for the first and the second case respectively. The evolution of the MAE as a function of polar angle, from the [001] to the [100] directions is shown in Fig. 4. The MAE for a general orientation of the magnetization is obtained from the total energy difference with respect to the energy corresponding to the magnetization lying along the dimers' direction, i.e. [001]. For both Ga distributions treated, the easy axis coincides with the orientation of the Ga pairs, that is the [001]. The value of the MAE for the system with a chain-like distribution is 5-6 times larger than the one obtained for the single

pairs B₂-like arrangement. If we compare the calculated results with ones obtained by us, we observe that the measured K_{PMA} values are between the MAE ones obtained for both calculated structures. The big difference between the values of the MAE obtained in the two situations analysed shows that the chemical ordering plays a critical role in the determination of K_{PMA} . Finally, these *ab initio* results represent a strong evidence pointing towards the conclusion that the experimentally observed PMA would arise from a preferential orientation of the Ga pairs along the z -axis, that is, perpendicular to the film plane.

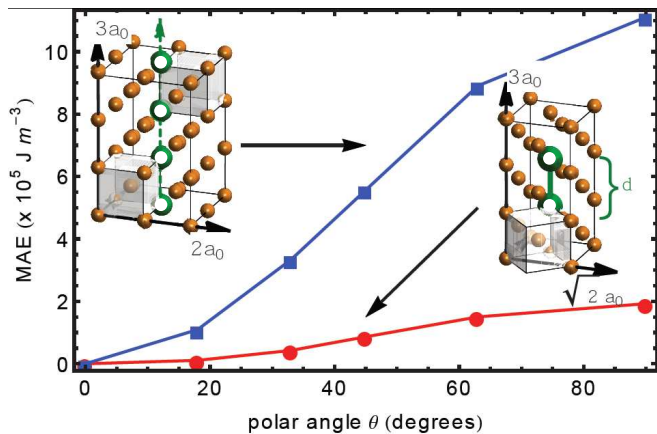


FIG. 4. (Color online) MAE as a function of the polar angle, θ , for both calculated structures. Large green (open) and small yellow (filled) symbols are Ga and Fe atoms, respectively.

IV. CONCLUSIONS

In conclusion, we have demonstrated the presence of a large PMA in $\text{Fe}_{1-x}\text{Ga}_x$ thin films grown on $\text{ZnSe}/\text{GaAs}(001)$, which is correlated to the tetragonal distortion reported in such films. The anisotropic distribution of Ga pairs along the sample appears as a possible origin of such a PMA. By performing *ab initio* calculations we show that an excess of such pairs along the perpendicular film plane direction provokes the PMA. In order to evaluate the Ga pairs contribution to the total magnetic anisotropy, we adopted a phenomenological approach similar to the model developed for bulk Galfenol,¹⁵ in which an additional energy term, that takes into account the preferential axis created by the Ga pairs, was introduced. We show that this Ga-pairs term is so important that a slight preference of Ga pairs to be aligned along the growth direction could lead to the observed K_{PMA} . Also, we have studied the in-plane anisotropies. On one hand, the magnetocrystalline one presents a similar behavior than the one observed in $\text{Fe}_{1-x}\text{Ga}_x$ bulk. On the other hand, the interfacial uniaxial anisotropy observed in Fe/ZnSe is also present in our samples. Finally, we show that $\text{Fe}_{1-x}\text{Ga}_x$ grown as thin film on $\text{GaAs}(001)$ becomes a potential material to be used in PMA-based devices, in which magnetostrictive and magnetic anisotropy are combined. This could open new perspectives to control PMA-related remarkable properties simply by strain.

ACKNOWLEDGMENTS

We thank to Dr. D. Sander and Prof. J. Kirschner for the help in magnetoelastic measurements, for valuable discussions and also for the careful reading of this manuscript. We acknowledge partial support from CONICET (PIP-00258), ANPCyT (PICT-2010-0773) and ANR (SPINSAW, ANR 13-JS04-0001-01).

- ¹ S. Mangin, D. Ravelosona, J. Katine, M. Carey, B. Terris, and E. Fullerton, *Nat. Mater.* **5**, 210 (2006).
- ² S. Yakata, H. Kubota, Y. Suzuki, K. Yakushiji, A. Fukushima, S. Yuasa, and K. Ando, *Appl. Phys. Lett.* **105**, 07D131 (2009).
- ³ B. D. Cullity and C. D. Graham, *Introduction to Magnetic Materials*, 2nd ed. (Wiley-IEEE Press, 2009).
- ⁴ S. Ikeda, K. Miura, H. Yamamoto, K. Mizunuma, H. Gan, M. Endo, S. Kanai, J. Hayakawa, F. Matsukura, and H. Ohno, *Nat. Mater.* **9**, 721 (2010).
- ⁵ E. Sallica Leva, R. C. Valente, F. Martinez Tabares, M. Vasquez Mansilla, S. Roshdestwensky, and A. Butera, *Phys. Rev. B* **82**, 144410 (2010).
- ⁶ B. Schulz and K. Baberschke, *Phys. Rev. B* **50**, 13467 (1994).
- ⁷ F. Vidal, Y. Zheng, P. Schio, F. J. Bonilla, M. Barturen, J. Milano, D. Demaille, E. Fonda, A. J. A. de Oliveira, and V. H. Etgens, *Phys. Rev. Lett.* **109**, 117205 (2012).
- ⁸ M. Hehn, S. Padovani, K. Ounadjela, and J. P. Bucher, *Phys. Rev. B* **54**, 3428 (1996).
- ⁹ Y. C. Chang, S. N. Hsiao, S. H. Liu, S. K. Chen, Y. T. Liu, H. Y. Lee, A. C. Sun, and J. G. Dhu, *J. Appl. Phys.* **115**, 17 (2014).
- ¹⁰ S. N. Piramanayagam and T. C. Chong, *Developments in Data Storage: Materials Perspective*, 1st ed. (John Wiley & Sons, 2011).
- ¹¹ O. Ivanov, L. Solina, V. Demshina, and L. Magat, *Phys. Met. Metallogr.* **35**, 81 (1973).
- ¹² T. Seki, S. Mitani, K. Yakushiji, and K. Takanashi, *Appl. Phys. Lett.* **88**, 172504 (2006).

- ¹³ D. Weller, A. Moser, L. Folks, M. Best, W. Lee, M. Toney, and M. Schwickert, IEEE T. Magn. **36**, 10 (2000).
- ¹⁴ We estimate that for lateral diameters below to ~ 130 nm, the PMA overcomes the demagnetizing field of a cylindrical ferromagnetic body. It can be obtained by comparing the analytical expression of the demagnetizing factor $N_z = \frac{1}{3}(\frac{4K_u}{\mu_0 M^2} + 1)$ with the ones tabulated in D.-X Chen, J. A. Brug, and R. B. Goldfarb IEEE Trans. Magn. **27**, 3601 (1991).
- ¹⁵ J. Cullen, P. Zhao, and M. Wuttig, J. Appl. Phys. **101**, 123922 (2007).
- ¹⁶ O. M. J. van't Erve, C. H. Li, G. Kioseoglou, A. T. Hanbicki, M. Osofsky, S.-F. Cheng, and B. T. Jonker, Appl. Phys. Lett. **91**, 122515 (2007).
- ¹⁷ D. Parkes, L. Shelford, P. Wadley, V. Holý, M. Wang, A. Hindmarch, G. Van Der Laan, R. Champion, K. Edmonds, S. Cavill, and A. Rushforth, Sci. Rep. **3**, 2220 (2013).
- ¹⁸ J. M. D. Coey, IEEE T. Magn. **47**, 4671 (2011).
- ¹⁹ M. Marangolo, F. Gustavsson, M. Eddrief, Ph. Saintcavit, V. H. Etgens, V. Cros, F. Petroff, J. M. George, P. Bencok and N. B. Brookes, Phys. Rev. Lett. **88**, 217202 (2002).
- ²⁰ M. Eddrief, M. Marangolo, V. H. Etgens, S. Ustaze, F. Sirotti, M. Mulazzi, G. Panaccione, D. H. Mosca, B. Lepine, and P. Schieffer, Phys. Rev. B **73**, 115315 (2006).
- ²¹ M. Eddrief, Y. Zheng, S. Hidki, B. Rache Salles, J. Milano, V. H. Etgens, and M. Marangolo, Phys. Rev. B **84**, 161410 (2011).
- ²² O. Kubaschewski, *Iron - Binary Phase Diagrams*, (Springer-Verlag, 1982).
- ²³ Y. Zhang and R. Wu, IEEE T. Magn. **47**, 4044 (2011).
- ²⁴ R. Wu, J. Appl. Phys. **91**, 7358 (2002).
- ²⁵ M. P. Ruffoni, S. Pascarelli, R. Grossinger, R. S. Turtelli, C. Bormio-Nunes, and R. F. Pettifer, Phys. Rev. Lett. **101**, 147202 (2008).
- ²⁶ M. Barturen, B. Rache Salles, P. Schio, J. Milano, A. Butera, S. Bustingorry, C. Ramos, A. J. A. de Oliveira, M. Eddrief, E. Lacaze, F. Gendron, V. H. Etgens, and M. Marangolo, Appl. Phys. Lett. **101**, 092404 (2012).
- ²⁷ M. Barturen, M. Sacchi, M. Eddrief, J. Milano, S. Bustingorry, H. Popescu, N. Jaouen, F. Sirotti, and M. Marangolo, Eur. Phys J. B **86**, 1 (2013).
- ²⁸ J. Smit and H. Beljers, Philips Res. Rep. **10**, 113 (1955).
- ²⁹ The resonance conditions during a FMR experiment depend on the magnetic anisotropy profile along the perpendicular directions respect to applied field at saturation. It allows us to determine the PMA even if the magnetic field is applied in the sample plane.
- ³⁰ E. Sjöstedt, L. Nordström, F. Gustavsson and O. Eriksson, Phys. Rev. Lett. **89**, 267203 (2002).
- ³¹ M. Marangolo, F. Gustavsson, G. M. Guichar, M. Eddrief, J. Varalda, V. H. Etgens, M. Rivoire, F. Gendron, H. Magnan, D. H. Mosca, and J. M. George, Phys. Rev. B **70**, 134404 (2004).
- ³² C. Kittel, Rev. Mod. Phys. **21**, 541 (1949).
- ³³ In order to determine ϵ_{zz} , we propose that deformation is driven by elastic forces and that the cell volume is preserved as experimentally observed in Ref. 21.
- ³⁴ J. Premper, D. Sander, and J. Kirschner, Rev. Sci. Instrum. **83**, 073904 (2012).
- ³⁵ D. Sander, Rep. Prog. Phys. **62**, 809 (1999).
- ³⁶ S. Tacchi, S. Fin, G. Carlotti, G. Gubbiotti, M. Madami, M. Barturen, M. Marangolo, M. Eddrief, D. Bisero, A. Rettori, and M. G. Pini, Phys. Rev. B **89**, 024411 (2014).
- ³⁷ By simple symmetry considerations, we can deduce how U_{pair}^0 corrects K_4^{Fe} . To do that we have to take into account that K_4 depends on the fourth power of direction cosines, as shown in Eq. (1), while U_{pair} is a summatory of terms that depend on α_i^2 . Then, to respect the K_4 four fold symmetry given by the direction cosines, the correction from U_{pair}^0 has to follow a $(\langle P_{0,i} \rangle K)^2$ dependence. Where $\langle P_{0,i} \rangle$ is the average of $P_{0,i}(R_i)$ over the all sites and it scales as x^2 , i.e. the probability to have a neighboring Ga atom (x) along the i -axis ($2x$) time a 1/2 factor in order to avoid double counting.
- ³⁸ H. Wang, Y. Zhang, R. Wu, L. Sun, D. Xu, and Z. Zhang, Sci. Rep. **3**, 3521 (2013).
- ³⁹ K. Schwarz and P. Blaha, Comp. Mater. Sci. **28**, 259 (2003), proceedings of the Symposium on Software Development for Process and Materials Design.
- ⁴⁰ The generalized gradient approximation (GGA) for the exchange and correlation potential in the PBE parametrization [J. P. Perdew, K. Burke and M. Ernzerhof, Phys. Rev. Lett **77**, 3865 (1996)] and the augmented plane waves local orbital (apw+lo) basis are used. The cutoff parameter is taken as $R_{mt}K_{max} = 7$, where K_{max} is the value of the largest reciprocal lattice vector used in the plane waves' expansion and R_{mt} is the smallest *muffin tin* radio. 8000 \vec{k} points in the Brillouin zone are enough to obtain an energy precision of 10^{-6} Ry, needed for the evaluation of the MAE. The unit cells of both calculated systems are shown in the insets of Fig. 4.